

$^{99m}\text{Tc-3P}_4\text{-RGD}_2$ radiotracers for SPECT/CT of esophageal tumor

GAO Shi¹ MA Qingjie¹ WEN Qiang¹ JIA Bing² LIU Zhaofei²
CHEN Zuowei³ ZHANG Haishan^{1,*} LI Dandan^{1,*}¹China-Japan Union Hospital, Jilin University, Changchun 130033, China²Medical Isotopes Research Center, Peking University, Beijing 100191, China³Department of Nuclear Medicine, People's Hospital of Shenzhen, Shenzhen 518020, China

Abstract In recent years, several RGD (Arg-Gly-Asp)-based radiotracers have already been successfully tested in human for the visualization of integrin $\alpha\beta_3$, demonstrating its feasibility in tumor diagnosis. In this paper, we evaluated the $^{99m}\text{Tc-3P}_4\text{-RGD}_2$ single photon emission computed tomography/computerized tomography (SPECT/CT) in patients suffering from space occupying disease of esophagus. 40 patients (34 males and 6 female; mean age: 58.3 years) with a suspected space occupying lesion of esophagus were included, thus finally obtaining their definite pathologic diagnosis (malignant, $n=32$; benign, $n=8$). All patients underwent endoscopic, barium esophagography and SPECT/CT imaging preoperatively. The chest SPECT was performed at 4 h after administration of $^{99m}\text{Tc-3P}_4\text{-RGD}_2$ with a dose of 939 ± 118 MBq. The diagnosis precision, sensitivity and specificity among these methods were compared. The relationship between radioactive uptake and clinical pathological stage of esophageal carcinoma was discussed by calculating the tumor to normal esophagus (T/N). Meanwhile, the integrin $\alpha\beta_3$ expression was assessed immunohistochemically in postoperative esophageal tissues. 31 patients were diagnosed as esophageal carcinoma; and 1, leiomyosarcoma; and 6, leiomyoma; and 2, esophageal tuberculosis. The accuracy, sensitivity and specificity of barium esophagography, endoscopic and SPECT/CT imaging are 92.5/93.8/87.5%, 97.5/96.9/100%, and 90/90.6/87.5%, respectively. Abnormal accumulation of radiotracer in 29 malignant lesions is observed. The SPECT/CT imaging displayed the region of radioactive uptake and lesions matched extremely with the T/N ratio from 1.31 to 2.79 (mean 2.04). A case with pulmonary metastases and a case with mediastinal lymph node metastases were found which were missed by barium esophagography and endoscopic. The $^{99m}\text{Tc-3P}_4\text{-RGD}_2$ uptake of the esophageal carcinoma masses had no relevance to the tumor pathologic classification ($P>0.05$). There was a significant positive correlation between T/N ratio and positive cell percentage of integrin $\alpha\beta_3$ ($r=0.976$), demonstrating the certain clinical potential in the diagnosis of esophageal carcinoma.

Key words $^{99m}\text{Tc-3P}_4\text{-RGD}_2$, Esophageal tumor, SPECT, Integrin $\alpha\beta_3$

1 Introduction

Esophageal carcinoma has a high morbidity and mortality. At present, FDG-PET as one of the most imaging techniques is widely applied to oncology. For esophageal carcinoma, the FDG-PET is used for detecting metastases and restaging recurrence evaluation, but not for local-regional disease^[1-3]. However, the high cost of FDG-PET limits its extensive applications in clinic.

Integrin $\alpha\beta_3$ is over-expressed on the tumor cells and the new blood vessels in a variety of tumors, such as glioblastomas, malignant melanomas and breast tumors^[4]. A close relevance between integrin $\alpha\beta_3$ expression and tumor metastases/angiogenesis has been investigated^[5-8]. There has been increasing interest in peptides containing the Arg-Gly-Asp (RGD) sequence for targeting of integrin $\alpha\beta_3$ to image malignant tumors. So far, most of the radiolabeled

Supported by National Natural Science Foundation of China (NSFC) projects (No.81271606) and Research Fund of Science and Technology Department of Jilin Province (No. 201015185 and No. 201201041) and the Research Fund of Shenzhen Sci-tech Department of Guangdong Province (No.201102154).

* Corresponding author. E-mail address: zhanghaishanmd@yahoo.com.cn, lidandan1979@hotmail.com

Received date: 2013-01-08

RGD containing agents were evaluated in animal models, and the only ^{18}F -Galacto-RGD and ^{18}F -AH111585 have been under clinical investigation for noninvasive visualization of integrin $\alpha\text{v}\beta\text{3}$ expression^[5-9]. Recently, a serial of investigations were performed on, as novel radioactive molecular probe, the $^{99\text{m}}\text{Tc}$ -3P₄-RGD₂ in xenografts tumor models was confirmed that it is very promising for the early detection of integrin $\alpha\text{v}\beta\text{3}$ -positive tumors^[10]. Also, the $^{99\text{m}}\text{Tc}$ -3P₄-RGD₂ could be easily prepared by freeze-dried kits with high labeling yield and radiochemical purity, thus exhibiting excellent *in vivo* behaviors in nonhuman primates^[11]. The clinical evaluations of $^{99\text{m}}\text{Tc}$ -3P₄-RGD₂ scintigraphy in lung tumor showed that it is promising for detecting lung malignancies^[12,13]. In this paper, we reported that the esophageal carcinomas was diagnosed by SPECT/CT with using the $^{99\text{m}}\text{Tc}$ -3P₄-RGD₂ in patients by SPECT/CT with 90% of accuracy. And to our surprise, a pulmonary metastases lesion and a mediastinal lymph node metastases lesion were found missed by barium esophagography and endoscopic were found in two cases, which were by SPECT/CT, demonstrating the SPECT/CT has advantages of endoscopic and barium esophagography were also demonstrated.

2 Materials and methods

2.1 Subjects

This clinical study was conducted between September 2009 and May 2012. 40 patients with suspected space occupying lesions (34 males and 6 females; age range: 38-82 years; mean age: 58.3 years), who were recruited from our hospital, not received any therapy including operation, chemotherapy and radiotherapy. Their pathologic diagnosis can be finally obtained. Approved by the local independent Ethics Committee and the Institutional Review Boards of China-Japan Union Hospital, Changchun, China, the novel radiotracer $^{99\text{m}}\text{Tc}$ -3P₄-RGD₂ was studied and applied. All patients signed the informed consent form. In addition to $^{99\text{m}}\text{Tc}$ -3P₄-RGD₂ SPECT/CT imaging, extra examinations, such as endoscopic and barium esophagography, were conducted in two weeks. The diagnosis standard was based on the pathology results after surgical operation and biopsy under endoscopic.

2.2 Methods

2.2.1 Radiopharmaceutical preparation

Provided by Medical Isotopes Research Center of Peking University, the $^{99\text{m}}\text{Tc}$ -3P₄-RGD₂ was prepared by freeze-dried kits adding Na^{99m}TcO₄ solution, the kit composition was mainly HYNIC-3P₄-RGD₂, and the procedures referred to the Ref.[12-14]. The quality control was conducted by radioactive thin layer chromatography (ITLC), counting the high labeling yield of about 95%.

2.2.2 Endoscopy

Endoscopy and suspicious tumor biopsy were performed by professionals of the two departments respectively. Similarly, a specialized pathologist was necessary. According to the pathological results, definite diagnosis should be conducted, the malignant lesions were signed as positive; and the benign lesions, as the negative.

2.2.3 Barium esophagography

The patients were examined in the upright position, and turned obliquely to the left. The esophagus in left posterior oblique, antero-posterior and right posterior oblique projections is viewed by continuous drinking of the barium suspension, presenting their functional changes and abnormal mucosal folds. The positive imaging features included ulcer, mucous layer interruption, esophageal wall rigidity, and localized filling defect. At least one specialized radiologist took part in the process.

2.2.4 SPECT/CT image acquisition

The patients received the $^{99\text{m}}\text{Tc}$ -3P₄-RGD₂ of 11.1 MBq (0.3 mCi)/kg by an intravenous injection. Data acquisition was performed by an integrated SPECT/CT system (PRECEDENCE Systems, Philip, Netherlands) in 4 h after injection. The scanner with dual-head-cameras used low-energy high-resolution collimators and a 20% energy window centered on 140 keV. The image acquisition was as follows. Chest CT scanning was performed with matrix of 256×256 and a 5-mm section thickness, and a SPECT emission scan, that covered the identical transverse field of view, was obtained (zoom, ×1, 30 s/frame/6°). Next, the image data sets were reconstructed iteratively by applying the CT data for attenuation correction. Finally, the coregistered images were displayed on a workstation.

In the scanning process, the patients were in the supine position, and the hands were laced behind head.

2.2.5 SPECT/CT image analysis

The images were assessed by a skilled radiologist and two experienced nuclear medicine physicians, who masked to the conditions of all the patients. The focus with $T/N > 1.2$ were considered as positive; and $T/N \leq 1.2$, negative. Once the positive lesion in the esophagus was definite, semi-quantification analysis of tumor uptake was obtained using T/N ratios, which were measured by region of interest (ROI) over the lesion located by CT. Similarly, the T/N ratios of the negative lesions were obtained by referring to endoscopy and barium meal.

2.2.6 Pathology and immunohistochemistry of integrin $\alpha\beta 3$ expression

At first, hematoxylin-eosin staining was used to define the pathological diagnosis. Immunohistochemical detection was used to examine the integrin $\alpha\beta 3$ expression of 40 esophageal tissue samples collected by operation or biopsy. The staining degree was scored as 0 (unstained); 1+ (faint yellow), 2+ (claybank), and 3+ (sepia). The number of tumor cells staining positive

at the surface membrane labeled as 4+ (>75%), 3+ (51–75%), 2+ (26–50%) and 1+ ($\leq 25\%$). When the above two grades are all equal or greater than 3, the positive is ensured.

Paraffin-embedded esophageal tumor tissue was stained by rabbit polyclonal anti-integrin $\alpha\beta 3$ antibody (1:300, Abbiotec, USA) as referred to the standard ABC method^[15].

2.2.7 Statistical analysis

All quantitative data were expressed as mean $\pm SD$, and parameters were evaluated by rank correlation analyses. T and χ^2 tests were performed by 5% level of statistical significance using SPSS (version 13.0).

2.3 Results

2.4 Clinical and pathological data

All of 40 lesions were identified by pathology, including 32 malignant cases (31 esophageal carcinomas and 1 leiomyosarcoma) and 8 benign cases (6 leiomyomas, 2 esophageal tuberculosis). The clinical and pathological information were listed as Table 1.

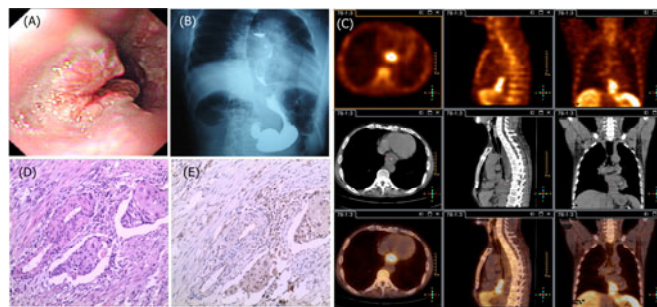


Fig.1 Esophageal cancer with the $^{99m}\text{Tc}-3\text{P}_4\text{-RGD}_2$ positive finding by the SPECT/CT scans. (A) A ulcerative tumor by endoscopy, (B) A localized filling defect by barium meal imaging, leading to lemostenosis, (C) High radiotracer uptake in the lesion, (D) A squamous cell carcinoma ($\times 100$) by histopathology staining, (E) A intense integrin $\alpha\beta 3$ expression by immunohistochemistry in both cancer cell and tumor vessels ($\times 100$).

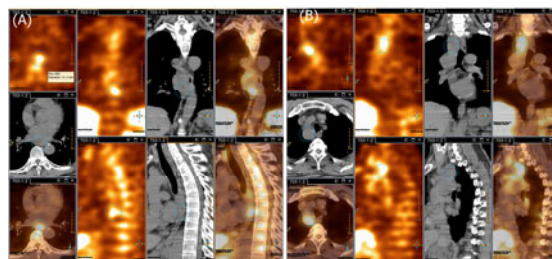


Fig.2 Esophageal cancer with mediastinal lymph node metastases. (A) High uptake of the radiotracer in the esophageal lesion, (B) Abnormal radioactivity accumulation in vena cava crypt of mediastinum.

Table 1 Patients with malignant and benign esophageal lesions

Patient	Pathology	Location	Clinical stage	T/N	Positive cell of $\alpha v\beta 3$ / %	Endoscopy	Barium meal	SPECT/CT
1	MD-SCC	Locusinferior	T ₃ N ₀ M ₀	1.31	11.28	+	+	+
2	MD-SCC	Locusmedilis	T ₃ N ₀ M ₀	1.37	12.65	+	+	+
3	MD-SCC	Locusmedilis	T ₃ N ₀ M ₀	1.47	11.78	+	+	+
4	MD-SCC	Locusmedilis	T ₄ N ₀ M ₀	2.56	23.74	+	+	+
5	PD-SCC	Locusinferior	T ₂ N ₀ M ₀	1.01	8.72	+	-	-
6	MD-SCC	Locusmedilis	T ₁ N ₀ M ₀	1.02	10.23	+	+	-
7	MD-SCC	Locusinferior	T ₂ N ₁ M ₀	2.75	27.64	+	+	+
8	MD-SCC	Locusinferior	T ₃ N ₁ M ₀	2.79	29.31	+	+	+
9	MD-SCC	Locusinferior	T ₃ N ₀ M ₀	2.77	28.19	+	+	+
10	PD-SCC	Locusinferior	T ₄ N ₁ M ₀	2.74	27.03	+	+	+
11	PD-SCC	Locusmedilis	T ₁ N ₀ M ₀	1.99	15.96	+	+	+
12	PD-SCC	Locusinferior	T ₃ N ₁ M ₁	2.04	17.63	-	+	+
13	WD-SCC	Locusmedilis	T ₁ N ₀ M ₀	1.02	9.91	+	+	-
14	MD-SCC	Locusinferior	T ₃ N ₁ M ₀	2.17	21.40	+	+	+
15	MD-SCC	Locusmedilis	T ₃ N ₁ M ₀	2.11	19.38	+	+	+
16	MD-SCC	Locussuperior	T ₃ N ₁ M ₀	1.75	13.45	+	+	+
17	PD-SCC	Locusmedilis	T ₃ N ₁ M ₀	2.07	18.31	+	+	+
18	PD-SCC	Locusmedilis	T ₃ N ₀ M ₀	2.22	21.92	+	+	+
19	WD-SCC	Locusmedilis	T ₃ N ₁ M ₀	2.41	23.66	+	+	+
20	MD-SCC	Locussuperior	T ₁ N ₀ M ₀	1.77	14.82	+	+	+
21	WD-SCC	Locusmedilis	T ₂ N ₁ M ₀	1.52	13.22	+	+	+
22	WD-SCC	Locusinferior	T ₃ N ₁ M ₀	2.59	25.18	+	+	+
23	WD-SCC	Locussuperior	T ₃ N ₀ M ₀	2.01	19.07	+	+	+
24	MD-SCC	Locusmedilis	T ₄ N ₁ M ₀	2.24	22.08	+	+	+
25	PD-SCC	Locusmedilis	T ₃ N ₀ M ₀	1.40	14.71	+	+	+
26	PD-SCC	Locusmedilis	T ₄ N ₁ M ₀	1.50	15.69	+	+	+
27	MD-SCC	Locusinferior	T ₃ N ₁ M ₀	1.63	15.33	+	+	+
28	MD-SCC	Locusmedilis	T ₄ N ₁ M ₀	2.03	19.62	+	+	+
29	WD-SCC	Locussuperior	T ₃ N ₁ M ₀	1.33	10.56	+	+	+
30	WD-SCC	Locusinferior	T ₃ N ₀ M ₀	2.19	21.58	+	+	+
31	MD-SCC	Locusinferior	T ₃ N ₁ M ₀	2.04	18.76	+	+	+
32	Leiomyosarcoma	Locusmedilis	/	1.62	17.30	+	-	+
33	Leimyoma	Locusmedilis	/	1.05	9.54	-	-	-
34	Leimyoma	Locusinferior	/	1.01	8.12	-	-	-
35	Leimyoma	Locusmedilis	/	1.10	10.63	-	-	-
36	Leimyoma	Locusmedilis	/	1.13	10.55	-	-	-
37	Leimyoma	Locusmedilis	/	1.00	8.79	-	-	-
38	Leimyoma	Locusinferior	/	1.05	7.42	-	-	-
39	Tuberculosis	Locusmedilis	/	1.73	12.83	-	+	+
40	Tuberculosis	Locusmedilis	/	1.08	9.18	-	-	-

Note: WD: Well-differentiated, MD : Moderate-differentiated , PD: Poor-differentiated , SCC: squamous cell carcinoma.

2.5 Scintimammography

In Fig.1, the SPECT/CT imaging shows that the radioactive uptake regions and lesions matched perfectly, while abnormal accumulations of radioactivity in 29 malignant lesions were observed. The T/N ratios were quantified from 1.31 to 2.79. The cases with multiple pulmonary and mediastinal lymph node metastases were further identified as squamous cell carcinoma by needle biopsy (Fig.2). The 3

carcinoma cases show no uptake of $^{99m}\text{Tc-3P}_4\text{-RGD}_2$, presenting a false negative imaging; and 1 tuberculosis case, abnormal uptake, a false positive imaging.

2.6 Comparison of endoscopy, barium meal and SPECT/CT imaging

The diagnostic performances of endoscopy, barium meal and SPECT/CT imaging were compared according to their accuracy, sensibility, specificity, positive and negative predictive value (PPV, NPV).

Table 2 shows that SPECT/CT imaging had the statistical significance to the others ($P>0.05$). 90.6% sensitivity and 87.5% specificity, having no

Table 2 Diagnostic performances of endoscopy, barium meal and SPECT/CT imaging

	Endoscopy	Barium meal	SPECT/CT	χ^2	P
Accuracy/%	97.5(39/40)	92.5(37/40)	90.0(36/40)	1.893	0.530
Sensitivity/%	96.9(31/32)	93.8(30/32)	90.6(29/32)	1.098	0.868
Specificity/%	100(8/8)	87.5(7/8)	87.5(7/8)	1.331	1.000
PPV/%	100(31/31)	96.8(30/31)	96.7(29/30)	1.287	0.770
NPV/%	88.9(8/9)	77.8(7/9)	70(7/10)	1.065	0.845

2.7 SPECT/CT imaging and clinicopathological features of esophageal cancer

The SPECT/CT imaging and clinicopathological features of esophageal carcinoma were studied, including invasion depth, differentiation and lymph node metastases. Table 3 shows that ^{99m}Tc -3P₄-RGD₂ uptake had no relevance to the tumor pathologic classification ($P>0.05$).

Table 3 Analysis between SPECT/CT imaging and clinicopathological parameters of esophageal cancer

	T/N	t	P
Invasion Depth			
T ₁ -T ₂	1.58±0.65	-1.752	0.090
T ₃ -T ₄	2.03±0.47		
Differentiation			
Well-differentiated(WD)	1.87±0.59	0.171	0.844
Moderate-differentiated(MD)	1.99±0.55		
Poor-differentiated(PD)	1.87±0.54		
Lymph Node Metastases			
Positive	2.10±0.46	-2.036	0.051
Negative	1.72±0.58		

2.8 Immunohistochemistry of integrin $\alpha\beta 3$ expression

Among the 32 esophageal malignant tumors, the 30 with positive integrin $\alpha\beta 3$ expression were confirmed in cell membrane and cytoplasm of cancer cells and tissue vessels where sepia grain could be seen. Also, 2 benign tumors with positive integrin $\alpha\beta 3$ expression were found, including the leiomyoma and tuberculosis samples. There was a significant positive correlation between T/N ratios and positive cell percentage of integrin $\alpha\beta 3$ expression ($r=0.976$).

3 Discussion

Though many esophageal carcinomas were conducted by the early detection and treatment, there is still a poor prognosis of their invasion and metastases

because the malignant biological behavior is inseparable from the neovascularization. It was confirmed that integrin $\alpha\beta 3$ plays a critical role in tumor-related angiogenesis and metastases^[16-19]. We showed that the ^{99m}Tc -3P₄-RGD₂ had the increased receptor binding affinity and improved kinetics for *in vivo* SPECT imaging of integrin $\alpha\beta 3$ expression in esophageal tumor.

Endoscopic and pathological techniques as standard clinically diagnosing esophageal tumors can provide important information for their differentiation and morphological change^[20]. Conventional imaging examinations, such as CT and barium esophagography, can reveal the tumor anatomic or morphological characteristics, but not the pathological features. The FDG-PET as a modality has the high sensitivity and accuracy for identifying distant metastasis in esophageal carcinoma, but it has the limitation because of high inspection cost^[21]. Recently, the ^{99m}Tc -3P₄-RGD₂ SPECT imaging was used to the solitary pulmonary nodule patients demonstrating a well differentiation of malignant and benign nodules^[12].

The accurate, sensitivity and specificity of barium esophagography, endoscopy and the ^{99m}Tc -3P₄-RGD₂ SPECT/CT imaging were 92.5/ 93.8/ 87.5%, 97.5/96.9/100% and, 90/90.6/87.5%. The SPECT/CT had no statistical significance to the other two examinations ($P>0.05$). In SPECT imaging, abnormal radioactivity accumulation in 29 malignant lesions could be observed. The combined SPECT/CT scans show that the regions between radioactive uptake and lesions matched extremely. 3 esophageal carcinoma cases with the sizes of less than 1.5 mm were not detected by the imaging. It is likely due to the low resolution of the imaging device^[22]. However, 2 case with metastases (1 case of pulmonary metastases and 1 case of mediastinal lymph node metastases) missed by

barium esophagography and endoscopy were successfully detected by the imaging.

In esophageal carcinoma cases, the *T/N* ratios show that the level of radioactive uptake had no relevance to the clinical stages and the malignancy degree. Among 31 esophageal carcinomas, 17 metastatic lymph nodes were located at one side of esophagus and left gastric arteria. There was no uptake in SPECT imaging. The first may be the high uptake of esophageal lesions and abdomen which can overlay the adjacent lymph nodes. The second is cardiac impulse and gastrointestinal motility. Then, the defects of the imaging devices cannot be ignored.

For immunohistochemistry study, the integrin $\alpha\beta3$ expressed highly in the malignant esophageal lesion tissues, primarily sepia grain in their cell membrane and cytoplasm and tissue vessels. There was a significant positive correlation between *T/N* ratios and integrin $\alpha\beta3$ expression. The imaging could provide vital reference to assess esophageal tumor characters and its neovascularization.

4 Conclusion

The accuracy, sensitivity and specificity of ^{99m}Tc - $3\text{P}_4\text{-RGD}_2$ SPECT/CT imaging are 90%, 90.6% and 87.5%, respectively. There was a significant positive correlation between *T/N* ratio and positive cell percentage of integrin $\alpha\beta3$. The accurate clinical information can be obtained, indicting that the imaging had a potential for diagnosing and detecting esophageal cancer. Increasing the samples and pathological types can further confirm the imaging feasibility for noninvasively monitoring tumor growth.

References

- 1 van Westreenen H L, Westerterp M, Bossuyt P M, *et al.* J Clin Oncol, 2004, **22**: 3805–3812.
- 2 van Vliet E P, Heijenbrok-Kal M H, Hunink M G, *et al.* Br

J Cancer, 2008, **98**: 547–557.

- 3 Deng S M, Zhang B, Wu Y W, *et al.* Nucl Sci Tech, 2011, **5**: 293–298.
- 4 Hynes R O. Cell, 1992, **69**: 11–25.
- 5 Haubner R, Weber W A, Beer A J, *et al.* P Lo S Med, 2005, **2**: e70.
- 6 Beer A J, Haubner R, Sarbia M, *et al.* Clin Cancer Res, 2006, **12**: 3942–3949.
- 7 Beer A J, Grosu A L, Carlsen J, *et al.* Clin Cancer Res, 2007, **13**: 6610–6616.
- 8 Ma Y F, Yu J F, Wang C, *et al.* Nucl Sci Tech, 2012, **1**: 47–51.
- 9 Kenny L M, Coombes R C, Oulie I, *et al.* J Nucl Med, 2008, **49**: 879–886.
- 10 Wang L J, Shi J Y, Kim Y S, *et al.* Mol Pharm, 2009, **6**: 231–245.
- 11 Jia B, Liu Z, Zhu Z, *et al.* Mol Imaging Biol, 2011, **13**: 730–736.
- 12 Ma Q, Ji B, Jia B, *et al.* Eur J Nucl Med Mol Imaging, 2011, **38**: 2145–2152.
- 13 Zhu Z H, Miao W B, Li Q W, *et al.* J Nucl Med, 2012, **53**: 1–7.
- 14 Cheng G H, Gao S, Ji T F, *et al.* Nucl Sci Tech, 2012, **6**: 349–354.
- 15 Chi V, Chandy K G. J Vis Exp, 2007, **8**: 308–318.
- 16 Plow EF, Haas TA, Zhang L, *et al.* J Biol Chem, 2000, **29**: 21785–21788.
- 17 Scatena M, Almeida M, Chaisson ML, *et al.* J Cell Biol, 1998, **4**: 1083–1093.
- 18 De S, Chen J, Narizhneva NV, *et al.* J Biol Chem, 2003, **40**: 39044–39050.
- 19 Rosa Hwang, MD, Judy Varner. Hematol Oncol Clin N Am, 2004, **5**: 991–1006.
- 20 Yerian L. Surg Oncol Clin N Am, 2009, **18**: 411–422.
- 21 Chin B B, Chang P P. Chang. Best Pract Res Clin Gastroenterol, 2006, **1**: 3–21.
- 22 Liu Y, Xie T W, Liu Q. Nucl Sci Tech, 2011, **3**: 165–173.